

Alma Mater Studiorum Università di Bologna
Archivio istituzionale della ricerca

Quantification of the errors associated with marker occlusion in stereophotogrammetric systems and implications on gait analysis

This is the final peer-reviewed author's accepted manuscript (postprint) of the following publication:

Published Version:

Conconi M., Pompili A., Sancisi N., Parenti-Castelli V. (2021). Quantification of the errors associated with marker occlusion in stereophotogrammetric systems and implications on gait analysis. JOURNAL OF BIOMECHANICS, 114, 1-9 [10.1016/j.jbiomech.2020.110162].

Availability:

This version is available at: <https://hdl.handle.net/11585/807718> since: 2024-05-09

Published:

DOI: <http://doi.org/10.1016/j.jbiomech.2020.110162>

Terms of use:

Some rights reserved. The terms and conditions for the reuse of this version of the manuscript are specified in the publishing policy. For all terms of use and more information see the publisher's website.

This item was downloaded from IRIS Università di Bologna (<https://cris.unibo.it/>).
When citing, please refer to the published version.

(Article begins on next page)

Journal of Biomechanics

Quantification of the Errors Associated with Marker Occlusion in Stereophotogrammetric Systems and implications on gait analysis

--Manuscript Draft--

Manuscript Number:	BM-D-20-00435R2
Article Type:	Full Length Article (max 3500 words)
Keywords:	Stereophotogrammetry; accuracy; marker occlusion; systematic error
Corresponding Author:	Michele Conconi University of Bologna Bologna, ITALY
First Author:	Michele Conconi
Order of Authors:	Michele Conconi Alessandro Pompili Nicola Sancisi Vincenzo Parenti-Castelli
Abstract:	<p>Optoelectronic stereophotogrammetric systems (OSSs) represent the standard for gait analysis. Despite widespread, their reported accuracy in nominal working conditions shows a variability of several orders of magnitude, ranging from few microns to several millimetres.</p> <p>No clear explanation for this variability has been provided yet. We hypothesized that this reflects an error affecting OSS outcomes when some of the tracked markers are totally or partially occluded. The aim of this paper is to quantify this error in static and dynamic conditions, also distinguishing between total and partial marker occlusion. A Vicon system featuring 8 cameras is employed in this study. Two camera distributions, one designed to maximize OSS accuracy and another one representative of a typical gait setup, are investigated. For both the setups, static and dynamic tests are performed, evaluating the different impact of partial and total marker occlusions. Marker occlusions significantly affected the system performances. The maximum measure variation reached 1.86 mm and 7.20 mm in static and dynamic conditions, respectively, both obtained in the case of partial occlusion. This systematic source of error is likely to affect gait measures: markers placed on the patient body are often visible only by half of the cameras, with swinging arms and legs providing moving occlusions. The maximum error observed in this study can potentially affect the kinematics outcomes of conventional gait models, particularly on frontal and coronal plane, and consequently the peak muscle forces estimated with musculoskeletal models.</p>

1 **Quantification of the Errors Associated with Marker Occlusion in**
2 **Stereophotogrammetric Systems and implications on gait analysis**

3 Michele Conconi¹, Alessandro Pompili¹, Nicola Sancisi¹, Vincenzo Parenti-Castelli¹.

4 ¹Dept. Of Industrial Engineering – DIN, University of Bologna, Italy.

5

6 Corresponding author:

7 Michele Conconi

8 Email: michele.conconi@unibo.it

9 Address: Viale del Risorgimento 2, 40139 Bologna, Italy

10 Tel: +39 051 20 93909

11 Fax: +39 051 20 93446

12

13 Keywords: Stereophotogrammetry, accuracy, marker occlusion, systematic error.

14

15 Word count: 3505/3500

1 ABSTRACT

2 Optoelectronic stereophotogrammetric systems (OSSs) represent the standard for gait analysis.
3 Despite widespread, their reported accuracy in nominal working conditions shows a variability of
4 several orders of magnitude, ranging from few microns to several millimetres.

5 No clear explanation for this variability has been provided yet. We hypothesized that this reflects an
6 error affecting OSS outcomes when some of the tracked markers are totally or partially occluded. The
7 aim of this paper is to quantify this error in static and dynamic conditions, also distinguishing between
8 total and partial marker occlusion.

9 A Vicon system featuring 8 cameras is employed in this study. Two camera distributions, one
10 designed to maximize OSS accuracy and another one representative of a typical gait setup, are
11 investigated. For both the setups, static and dynamic tests are performed, evaluating the different
12 impact of partial and total marker occlusions.

13 Marker occlusions significantly affected the system performances. The maximum measure variation
14 reached 1.86 mm and 7.20 mm in static and dynamic conditions, respectively, both obtained in the
15 case of partial occlusion. This systematic source of error is likely to affect gait measures: markers
16 placed on the patient body are often visible only by half of the cameras, with swinging arms and legs
17 providing moving occlusions. The maximum error observed in this study can potentially affect the
18 kinematics outcomes of conventional gait models, particularly on frontal and coronal plane, and
19 consequently the peak muscle forces estimated with musculoskeletal models.

20

1 INTRODUCTION

2 Optoelectronic stereophotogrammetric systems (OSSs) emerged in the 1980s and became the
3 standard for gait analysis in the 1990s (Baker et al., 2017). Recently, OSSs found application also in
4 robotics (Manecy et al., 2015; Morozov et al., 2016).

5 Despite the many applications, OSS accuracy is still undetermined, the literature reporting values
6 ranging from a few microns to several millimetres (table 1). In part, this variability depends on the
7 different definitions of accuracy (Eichelberg et al., 2016), and the specific OSSs (Ehara et al., 1997;
8 Richards, 1999). Also, OSS accuracy changes within the calibrated volume (CV) (Windolf et. al,
9 2008; Yang et al., 2012; Eichelberg et al., 2016; Aurand et al., 2017), it is related to camera number
10 and distribution (Miller et al., 2002; Windolf et. al, 2008; Eichelberg et al., 2016; Aurand et al., 2017),
11 to marker size (Liu et al., 2007; Windolf et. al, 2008; Yang et al., 2012; Diaz Novo et al., 2014;
12 Merriaux et al., 2017), velocity (Diaz Novo et al., 2014; Di Marco et al., 2017; Merriaux et al., 2017)
13 and calibration technique (Windolf et. al, 2008; Yang et al., 2012; Di Marco et al., 2017). None of
14 these factors, however, directly explained the several millimetres of variation observed in OSS
15 accuracy even in nominal working conditions. A possible explanation may come from the OSS
16 tracking process. Marker location is determined as the intersection of all the camera tracking rays.
17 Due to measurement errors, these rays are skew and do not meet at a single point. The location of a
18 marker is thus the point that minimizes the distance from all the tracking rays (Josefsson et al., 1996).
19 The total or partial occlusion of a marker with respect to one or more cameras changes the set of
20 tracking rays. This sudden change introduces a discontinuity in the reconstructed marker position and
21 a consequent apparent marker displacement, hereinafter called *marker-occlusion-artefact* (MOA).
22 Despite the wide literature on the topic and the general acknowledgement of implication of marker
23 occlusion, only two papers directly addressed the MOA. Richards (1999) unintentionally created an
24 experiment in which markers were both partially and totally occluded. Markers were mounted on a
25 rotating plate so that they were visible by different camera subsets featuring no more than 3 cameras

at a time. The transition between subsets necessarily implies both types of occlusions. The maximum inter-marker distance (IMD) error was 5.57 mm for the most accurate OSS, ascribed to the reduction in the number of tracking cameras. Later investigations showed however that the impact of camera number on the system accuracy is at least one order of magnitude smaller (Miller et al., 2002; Eichelberg et al., 2016). Kuxhaus and co-workers (2009) addressed MOA by investigating the effect of occluding some cameras. The study, however, did not provide a complete analysis of MOA, particularly of partial occlusion, also lacking a sound explanation and a quantification of MOA in dynamic conditions.

We hypothesized that MOA may result in considerable errors, explaining the observed variability in OSS performances. The paper aims to verify this hypothesis and to provide a quantification of MOA, both for total and partial occlusion. First, the impact of the camera number on the OSS accuracy is evaluated, to isolate this effect from the MOA. Then, a static test is performed to enlighten the effect of partial and total marker occlusions in controlled conditions. Finally, a dynamic test mimicking gait conditions is performed to quantify the MOA in a typical scenario. In this latter case, data filtering is also applied to evaluate the possible mitigation of MOA.

METHODS

Note: Supplementary material is denoted by S.

Experimental setups

We used a Vicon system (6 Bonita, 2 Vero cameras), processing data within Nexus 2.5, keeping all system settings at default values. The experiments were performed in a laboratory with concrete-ground floor. Cameras were warmed up more than 2.5 hours to stabilize operating temperature. Calibration was performed by sweeping the Vicon active wand in the entire CV, using at least 3000 frames per camera. Maximum and mean values of Vicon Nexus world errors are reported in

1 supplementary material. Acquisitions were performed at 100 Hz, using Polaris retro-reflective
2 passive markers, 11.5 mm in diameter. Marker centroid was computed by the Vicon circular fitting,
3 using the standard 0.5 threshold value. The minimum number of tracking cameras to reconstruct a
4 marker was set to 3.

5 We tested two camera distributions. The first one (measure setup) was defined to maximize the
6 system accuracy (Windolf et. al, 2008): cameras were evenly distributed on a circular arch, concentric
7 with the CV centre, symmetrically varying their heights (figure 1.a). The second camera distribution
8 (gait setup) is typical of gait laboratories. Cameras were distributed on a rectangle, concentric with
9 the CV and with standard dimensions (Eichelberg et al., 2016) scaled proportionally to marker size
10 (figure 1.b).

11 A cross-shaped object featuring a cluster of markers was used during tests (figure 2.a). Reference
12 IMDs were measured with a laser scanner (Faro CAM2 ScanArm, accuracy ± 0.025 mm). For the
13 sake of concision, only results related to markers M1 and M2 in figure 2.a (IMD: 142.62 mm) are
14 reported in the main text. To evaluate the possible impact of the reference IMD value, an additional
15 marker pair was considered in the additional material (IMD: 605.37 mm, Figure S2).

16

17 *OSS accuracy quantification*

18 This test aims at quantifying variation in OSS accuracy with the number of cameras. We adopted a
19 standard approach (table 1), defining accuracy as the mean absolute error between OSS-measured
20 and laser-evaluated IMDs.

21 After OSS calibration, the tracking object was placed in the CV centre, facing upward. All markers
22 were fully visible to all cameras and were not moved during the experiment. A first acquisition was
23 taken with all cameras. Then, six acquisitions were taken using different camera subsets, each time
24 occluding some cameras with a paper foil, carefully positioned by hand. The different camera subsets

1 are reported in table S1. To verify whether the overall process altered the system calibration, a final
2 acquisition was taken, again with all cameras. Each acquisition lasted 10 seconds and marker
3 coordinates were defined as the average values over this period. The process was repeated 5 times,
4 each time recalibrating the system.

5 Statistical analysis was performed on average values from each trial. Initial (5 values), occluded (30
6 values), and final (5 values) OSS accuracies were compared by one-way ANOVA (significance:
7 $p \leq 0.05$), followed by Bonferroni's post-hoc tests.

8

9 *Static quantification of MOA*

10 In static condition, MOA was evaluated as the norm of absolute marker displacement induced by the
11 occlusion with respect to a reference position measured with the contribution of all cameras. With the
12 tracking object in the CV centre, a first acquisition was taken with no occlusions. Subsequent
13 acquisitions were taken each time physically occluding the view of marker M2 to a camera subset
14 (table S1) with a wooden obstacle, first partially and then totally (figure S1), for a total of 12
15 acquisitions. The partial occlusion was set to the limit of marker centroid reconstruction under the
16 chosen circularity threshold of 0.5. A final acquisition was taken with no occlusions. Each acquisition
17 lasted 10 seconds and the coordinates of marker M2 were defined as the average values over this
18 period. The process was repeated 5 times, each time recalibrating the system. For each acquisition,
19 marker displacement was defined as the difference with respect to the first acquisition. System
20 repeatability was defined as the difference in the marker location between initial and final acquisition
21 with no occlusion.

22 Statistical analysis was performed on average values from each trial. System repeatability (5 values)
23 and marker displacement associated with total (30 values) and partial (30 values) occlusions were
24 compared by one-way ANOVA (significance: $p \leq 0.05$), followed by Bonferroni's post-hoc tests.

1

2 *Dynamic quantification of MOA*

3 The dynamic impact of MOA was evaluated through IMD errors. The tracking object was mounted
4 on a rotor with horizontal axis, defining a pendulum, positioned in the CV centre with the axis aligned
5 with a plane of symmetry of the two camera distributions (figure 1). In the gait setup, cameras 6, 7,
6 and 8 were always partially or totally occluded, replicating the conditions of gait measurement, where
7 cameras on the left cannot see markers on the right of the patient.

8 The pendulum was rotated manually at 90° with respect to the resting position and then released,
9 allowing free oscillations. The pendulum motion was acquired until it stopped, after approximatively
10 two minutes. The test was then repeated after placing an obstruction between the pendulum and the
11 cameras (figure 2.b). The pendulum motion with respect to the obstruction resulted in total, partial or
12 no occlusion of marker M2 at different times for different cameras. Five trials were acquired for both
13 tests.

14 The mean IMD absolute error (MIMDAE) was computed for each trial. To estimate the maximum
15 uncertainty in the IMD measure, the maximum IMD variation was also computed for each trial. To
16 distinguish between the contribution of total and partial marker occlusions, for both camera setups
17 the single pendulum oscillation (i.e. half period) showing the maximum IMD variation over all trials
18 was manually analysed. Data were divided into two groups, one featuring at least one partial occlusion
19 (36 and 23 measurements for the measure and the gait setup, respectively), the other featuring only
20 total occlusions (41 and 38 measurements for the measure and the gait setup, respectively). This
21 required an operator to inspect each frame recorded by each camera, making it unpracticable to extend
22 the analysis to all the occluded trials.

23 Finally, to evaluate the impact of filtering, MIMDAEs and maximum variations were computed
24 applying a low-pass zero-lag fourth-order Butterworth digital filter with two cut-off frequencies, i.e.

4.5 Hz (Ren et al., 2008) and 15 Hz (Fregly et al., 2012). The Nexus pattern-fill algorithm was applied to the trajectory of marker M2 before filtering, taking marker M1 as the donor, to avoid time discontinuity, which could affect the filter outcome.

Un-occluded (5 values), occluded (5 values), and filtered (two groups of 5 values each) MIMDAEs were compared through one-way ANOVA (significance: $p \leq 0.05$), followed by Bonferroni's post-hoc tests. The same procedure was repeated for the additional marker pair (Fig. S2).

Un-occluded MIMDAEs were also compared with partially and totally occluded IMD errors for the single oscillations through one-way ANOVA (significance: $p \leq 0.05$), followed by Bonferroni's post-hoc tests.

RESULTS

All details about post-hoc tests are reported in tables S2-S5.

No statistical differences were found in system accuracy with and without occluded cameras. Similarly, no statistical difference was observed between initial and final acquisition with all cameras. Overall, the accuracy of the two camera setups was below 0.08 ± 0.01 mm when all cameras contributed to tracking, and below 0.11 ± 0.07 mm in case of occlusion (table 2).

In the static tests, system repeatability was 0.12 ± 0.07 and 0.07 ± 0.04 mm for the measure and the gait setup, respectively. The absolute marker displacement induced by MOA in case of marker total occlusion was not statistically different from the system repeatability for the measure setup ($p > 0.2$), always remaining below 0.16 ± 0.09 mm (table 3). Conversely, in the gait setup the marker displacement due to total marker occlusion significantly exceeded the system repeatability ($p < 0.005$), the value being 0.18 ± 0.10 mm. For both setups, partial marker occlusions significantly exceeded both total occlusion and system repeatability ($p < 0.001$), reaching an average displacement of 0.78 ± 0.43 mm and 1.21 ± 0.25 mm for the measure and the gait setup, respectively. For the measure setup, maximum displacement reached 0.44 mm for total occlusion and 1.73 mm for partial occlusion. For

the gait setup, maximum displacement reached 0.47 mm for total occlusion and 1.86 mm for partial occlusion.

In figure 3, the IMD errors obtained in un-occluded, occluded, and filtered dynamic tests are plotted versus the pendulum rotation angle. In the un-occluded tests, the MIMDAE stayed always below 0.09 ± 0.00 mm while the maximum IMD variation reached 0.20 mm and 0.83 mm for the measure and the gait setup, respectively (table 4). Occlusions significantly increase the MIMDAE ($p < 0.001$), which reached 0.26 ± 0.01 mm and 0.18 ± 0.01 mm, with maximum IMD variation of 7.20 mm and 5.81 mm for the measure and the gait setup, respectively. The second pair of markers showed similar values despite the higher IMD reference value, maximum IMD variation during occluded motion being 7.03 and 5.67 mm for the measure and gait setup, respectively (Table S6). Filtering significantly reduced the MIMDAE ($p < 0.001$) and maximum IMD variation for the measure setup, with 4.5 Hz cut-off frequency resulting the most efficient (table 4). On the contrary, filtering increased the MIMDAE for the gait setup ($p < 0.001$), 15 Hz cut-off frequency also increasing the maximum IMD variation to 6.21 mm (table 4).

In figure 4, the single oscillations were analysed. With respect to un-occluded motion, total occlusions significantly increased the MIMDAE to 0.16 ± 0.13 mm and 0.18 ± 0.24 mm ($p < 0.001$), with a maximum IMD variation of 1.05 mm and 1.52 mm, for the measure and the gait setup, respectively (table 5). Partial occlusions further increased the MIMDAE to 0.56 ± 0.60 mm and 0.46 ± 0.78 mm ($p < 0.001$), with a maximum IMD variation of 4.47 mm and 4.94 mm, for the measure and the gait setup, respectively.

DISCUSSION

1 A source of error is analysed, which systematically affects OSSs when the view of a marker is totally
2 or partially occluded to some cameras in the system. This effect is denoted as marker occlusion
3 artefact (MOA).

4 MOA does not seem to originate from the number of tracking cameras. Camera occlusion did not
5 significantly affect OSS accuracy, whose values are well in agreement with the literature (Eichelberg
6 et al., 2016). The camera number provides thus a minor contribution to MOA.

7 The change of tracking camera subset (and thus tracking rays) due to occlusions has a considerable
8 effect, even when tracking still markers laying at the centre of the CV. In these conditions, marker
9 total occlusion results in an apparent marker displacement which is higher than the OSS repeatability
10 (peak value: 0.47 mm). Marker partial occlusion has a significantly higher impact, with a peak
11 apparent displacement of 1.73 mm and 1.86 mm for the measure and gait setup, respectively. These
12 values are relevant, since have been obtained in strictly controlled conditions, aimed at minimizing
13 the errors.

14 In dynamic conditions, MOA effects are amplified, the maximum IMD variation reaching 7.20 mm
15 and 5.82 mm for the measure and the gait setup, respectively, while un-occluded maximum IMD
16 variation remains below 1 mm. Similar values are found in the literature (below 2 mm, Di Marco et
17 al., 2017; Merriaux et al., 2017), although a direct comparison is hard due to the different error
18 definitions. The single oscillations analysis showed that total and partial occlusions provide
19 significantly different errors: maximum IMD variation reached 1.52 mm and 4.94 mm for total or
20 partial marker occlusions, respectively, both obtained with the gait setup. The small differences
21 between occluded and un-occluded MIMDAEs deserve a discussion. During occluded tests different
22 conditions take place (total, partial and no occlusion). The final MIMDAE reflects the ratio among
23 these events, rather than the mean error associated with occlusion. Thus, MIMDAE can be used to
24 discriminate between experiments but, in terms of MOA quantification, maximum IMD variation is
25 more significant.

1 The IMD value has a minor effect on the error. The two considered marker pairs showed similar IMD
2 variation, despite the very different IMD. The observed errors are thus not a percentage of the
3 reference distance, rather it results from an apparent displacement of the solely occluded marker M2.

4 According to the setup and the cut-off frequency, Butterworth filters may reduce or amplify the effects
5 of MOA. This may be explained considering that Butterworth filtering works on time while MOA
6 depends on the marker displacement relative to an occlusion, therefore having a geometrical nature
7 not directly related to time. As a confirmation, comparing figures 2b and 3, IMD error changes with
8 the pendulum position, with peak values obtained at angles corresponding to marker M2 passing
9 behind the obstruction. Traditional filtering strategies should therefore be considered carefully: in
10 case of possible partial occlusion over multiple frames, Butterworth filtering is not recommended. If
11 strictly needed, the present analysis suggests better performances for the 4.5 Hz cut-off frequency.

12 The present analysis confirms the original hypothesis that a discontinuity in the set of tracking rays
13 due to total or partial occlusions may result in apparent marker displacement of significant amplitude.
14 This explanation is also compatible with partial occlusions being the main source of error. In this
15 case, in fact, some tracking rays are misoriented, no longer passing through the real marker centre,
16 but still contributing to tracking. In total occlusion, instead, the set of tracking rays changes but the
17 remaining rays are still oriented correctly, thus resulting in smaller errors. We couldn't find any
18 straight relation between the number of occluded and partially-occluded cameras and the error when
19 analysing single oscillations, although a deeper investigation would be deserved. The quantification
20 of MOA here presented is consistent with the previous literature: all studies with a constant and full
21 visibility of markers reported accuracies and maximum errors well below one millimetre (Miller et
22 al., 2002; Liu et al., 2007; Windolf et. al, 2008; Yang et al., 2012). On the contrary, studies in which
23 markers may have been occluded during experiments showed maximum errors consistent to our
24 results (Ehara et al., 1997; Richards, 1999; Diaz Novo et al., 2014; Eichelberg et al., 2016).

1 MOA is likely to affect gait measures, since markers are placed on the side of the subject, thus facing
2 half the cameras, with swinging arms and legs providing moving occlusions. Partial and total marker
3 occlusion may simultaneously take place for different markers thus resulting also in deformation of
4 the cluster and further amplification of the overall error. Reasonably, MOA was included so far within
5 the more evident soft tissue artefact (STA) and its impact was not recognized. MOA depends on the
6 relative motion between the marker and the source of occlusion and therefore it has a systematic
7 nature (figure 3), which however may change considerably from task to task or between individuals.
8 In this perspective, MOA may contribute to explain the reported variability between gait
9 measurements (McGinley et al., 2009) and the difficulty in producing an effective model for the STA
10 (Dumas et al., 2014; Cereatti et al., 2017).

11 A measure uncertainty of 7.20 mm on the single marker clearly reduces the reliability of OSSs as
12 measurement systems per se, e.g., in robotics or other applications tracking rigid bodies. Its impact
13 on gait analysis, however, deserves to be discussed. Using the conventional gait model (Baker et al.,
14 2017), errors of similar amplitude induced up to 8° error on the shank axial rotation (Holden et al.,
15 1997). Some researchers concluded that these errors would not likely affect the clinical interpretation
16 of data (Holden et al., 1997; Manal et al., 2002), while others consider them large enough to mislead
17 clinical interpretation (McGinley et al., 2009), particularly when results on the frontal and axial plane
18 are considered (Stagni et al., 2005). Measured kinematics is also used to compute inverse dynamics,
19 quite sensitive to errors in joint kinematics (Riemer et al., 2008). Multibody kinematic optimization
20 may reduce (Leardini et al., 2017) but not eliminate (Lamberto et al., 2017, Martelli et al., 2020) the
21 impact of measurement errors on kinetic outcomes of musculoskeletal models. Overall, it is
22 reasonable that MOA impacts on gait analysis outcomes, particularly when investigating pathological
23 gait, whose abnormalities mainly occur on frontal and axial planes (Gage, 1991). A thorough
24 investigation is however needed.

The present analysis has limitations. The experiment for dynamic quantification of MOA is a simplification designed to mimic marker occlusions on a swinging limb: the MOA impact on data from gait analysis remains to be determined. Only two camera setups were considered and the effects of MOA for different subsets of occluded cameras were aggregated. A thorough investigation of MOA dependence from the camera distribution, although interesting, would require establishing a correlation among several parameters of each camera setup, which is beyond the aims of the present paper. Software parameters were kept at default values. Since some of them (e.g. minimum circularity) may impact the measure, a deeper investigation would be of interest. Only one OSS was investigated: the same analysis with different OSSs could verify the generality of the problem. Preliminary investigations suggest however that the present analysis still holds for higher-end cameras within the same OSS, and for other OSSs. Finally, the dynamic effects of MOA were evaluated by means of relative displacements. The values here reported represent therefore a lower limit: any displacement that preserves the IMD distance did not contribute to the error.

CONCLUSION

Marker occlusion results in a systematic artefact affecting optoelectronic stereophotogrammetric systems. This investigation shows that when the calibrated set of cameras tracking a marker does not change, the maximum error stays below one millimetre. Conversely, in case of occlusion, an apparent marker displacement up to 7.20 mm may occur. Partial occlusion is more critical than total occlusion, both exceeding the effects of a reduction in the number of tracking cameras. Errors of this magnitude may potentially affect the kinematics outcomes of gait analysis, particularly on the frontal and axial plane, and the peak muscle forces estimated with standard musculoskeletal models.

REFERENCES

- [1] Aurand, A. M., Dufour, J. S., Marras, W. S., 2017. Accuracy map of an optical motion capture system with 42 or 21 cameras in a large measurement volume. *Journal of Biomechanics* 58, 237–240.
- [2] Baker, R., Leboeuf, F., Reay, J., Sangeux, M., 2017. The Conventional Gait Model-Success and Limitations. In: *Handbook of Human Motion*. Cham: Springer International Publishing, pp. 489-508.
- [3] Cereatti, A., Bonci, T., Akbarshahi, M., Aminian, K., Barré, A., Begon, M. et al., 2017. Standardization proposal of soft tissue artefact description for data sharing in human motion measurements. *Journal of Biomechanics* 62, 5-13.
- [4] Clément, J., Dumas, R., Hagemester, N., De Guise, J. A., 2015. Soft tissue artifact compensation in knee kinematics by multi-body optimization: performance of subject-specific knee joint models. *Journal of Biomechanics*. 48, 3796-3802.
- [5] Di Marco, R., Rossi, S., Castelli, E., Patani, F., Mazza, C., Cappa, P., 2017. Effects of the calibration procedure on the metrological performances of stereophotogrammetric systems for human movement analysis. *Measurement* 101, 265–271.
- [6] Diaz Novo, C., Alharbi, S., Fox, M., Ouellette, E., Biden, E., Tingley, M. et al., 2014. The impact of technical parameters such as video sensor technology, system configuration, marker size and speed on the accuracy of motion analysis systems. *Ingeniería Mecánica, Tecnología y Desarrollo* 5, 265–271.
- [7] Dumas, R., Camomilla, V., Bonci, T., Cheze, L., Cappozzo, A., 2014. Generalized mathematical representation of the soft tissue artefact. *Journal of Biomechanics* 47, 476-481.
- [8] Ehara, Y., Fujimoto, H., Miyazaki, S., Mochimaru, M., Tanaka, S., Yamamoto, S., 1997. Comparison of the performance of 3D camera systems II. *Gait & Posture* 5, 251-255.
- [9] Eichelberger, P., Ferraro, M., Minder, U., Denton, T., Blasimann, A., Krause, F. et al., 2016. Analysis of accuracy in optical motion capture - A protocol for laboratory setup evaluation. *Journal of Biomechanics* 49, 2085-2088.
- [10] Fregly, B. J., Besier, T. F., Lloyd, D. G., Delp, S. L., Banks, S. A., Pandy, M. G. et al., 2012. Grand challenge competition to predict in vivo knee loads. *Journal of Orthopaedic Research* 30, 503-513.
- [11] Gage, J. R., 1991. Gait analysis in cerebral palsy. *Clinics in Developmental Medicine* 121.
- [12] Holden, J. P., Orsini, J. A., Siegel, K. L., Kepple, T. M., Gerber, L. H., Stanhope, S. J., 1997. Surface movement errors in shank kinematics and knee kinetics during gait. *Gait & Posture* 5, 217-227.
- [13] Josefsson, T., Nordh, E., Eriksson, P.-O., 1996. A flexible high-precision video system for digital recording of motor acts through lightweight reflex markers. *Computer Methods and Programs in Biomedicine* 49, 119-129.
- [14] Kuxhaus, L., Schimoler, P. J., Viperman, J. S., Miller, M. C., 2009. Effects of camera switching on fine accuracy in a motion capture system. *Journal of Biomechanical Engineering* 131, 014502-8.

- [15] Lamberto, G., Martelli, S., Cappozzo, A., Mazza, C., 2017. To what extent is joint and muscle mechanics predicted by musculoskeletal models sensitive to soft tissue artefacts?. *Journal of Biomechanics* 62, 68-76.
- [16] Leardini, A., Belvedere, C., Nardini, F., Sancisi, N., Conconi, M., Parenti-Castelli, V., 2017. Kinematic models of lower limb joints for musculo-skeletal modelling and optimization in gait analysis. *Journal of Biomechanics* 62, 77-86.
- [17] Liu, H., Holt, C., Evans, S., 2007. Accuracy and repeatability of an optical motion analysis system for measuring small deformations of biological tissues. *Journal of Biomechanics* 40, 210-214.
- [18] Manal, K., McClay, I., Richards, J., Galinat, B., Stanhope, S., 2002. Knee moment profiles during walking: errors due to soft tissue movement of the shank and the influence of the reference coordinate system. *Gait & Posture* 15, 10-17.
- [19] Manecy, A., Marchand, N., Ruffier, F., Viollet, S., 2015. X4-mag: a low-cost open-source micro-quadrotor and its linux-based controller. *International Journal of Micro Air Vehicles* 7, 89-109.
- [20] Martelli, S., Sancisi, N., Conconi, M., Pandy, M. G., Kersh, M. E., Parenti-Castelli, V., & Reynolds, K. J., 2020. The relationship between tibiofemoral geometry and musculoskeletal function during normal activity. *Gait & Posture* 80, 374-382.
- [21] McGinley, J. L., Baker, R., Wolfe, R., Morris, M. E., 2009. The reliability of three-dimensional kinematic gait measurements: a systematic review. *Gait & Posture* 29, 360-369.
- [22] Meriaux, P., Dupuis, Y., Bouteau, Ré., Vasseur, P., Savatier, X., 2017. A study of Vicon system positioning performance. *Sensors* 17, 1591.
- [23] Miller, C., Mulavara, A., Bloomberg, J., 2002. A quasi-static method for determining the characteristics of a motion capture camera system in a “split-column” configuration. *Gait & Posture* 16, 283-287.
- [24] Morozov, M., Riise, J., Summan, R., Pierce, S. G., Mineo, C., MacLeod, C. N. et al., 2016. Assessing the accuracy of industrial robots through metrology for the enhancement of automated non-destructive testing. In *Multisensor Fusion and Integration for Intelligent Systems (MFI)*, IEEE International Conference, 335-340.
- [25] Ren, L., Jones, R. K., Howard, D., 2008. Whole body inverse dynamics over a complete gait cycle based only on measured kinematics. *Journal of Biomechanics* 41, 2750-2759.
- [26] Richards, J. G., 1999. The measurement of human motion: A comparison of commercially available systems. *Human Movement Science* 18, 589-602.
- [27] Riemer, R., Hsiao-Weeksler, E. T., Zhang, X., 2008. Uncertainties in inverse dynamics solutions: a comprehensive analysis and an application to gait. *Gait & Posture* 27, 578-588.
- [28] Stagni, R., Fantozzi, S., Cappello, A., Leardini, A., 2005. Quantification of soft tissue artefact in motion analysis by combining 3D fluoroscopy and stereophotogrammetry: a study on two subjects. *Clinical Biomechanics* 20, 320-329.

- 1 [29] Windolf, M., Götzen, N., Morlock, M., 2008. Systematic accuracy and precision analysis of
2 video motion capturing systems-exemplified on the Vicon-460 system. Journal of
3 Biomechanics. 41, 2776-2780.
- 4 [30] Yang, P.F., Sanno, M., Brüggemann , G.P., Rittweger, J., 2012. Evaluation of the
5 performance of a motion capture system for small displacement recording and a discussion
6 for its application potential in bone deformation in vivo measurements. Proceedings of the
7 Institution of Mechanical Engineers, Part H: Journal of Engineering in Medicine 226, 838-
8 847.

FIGURE CAPTIONS

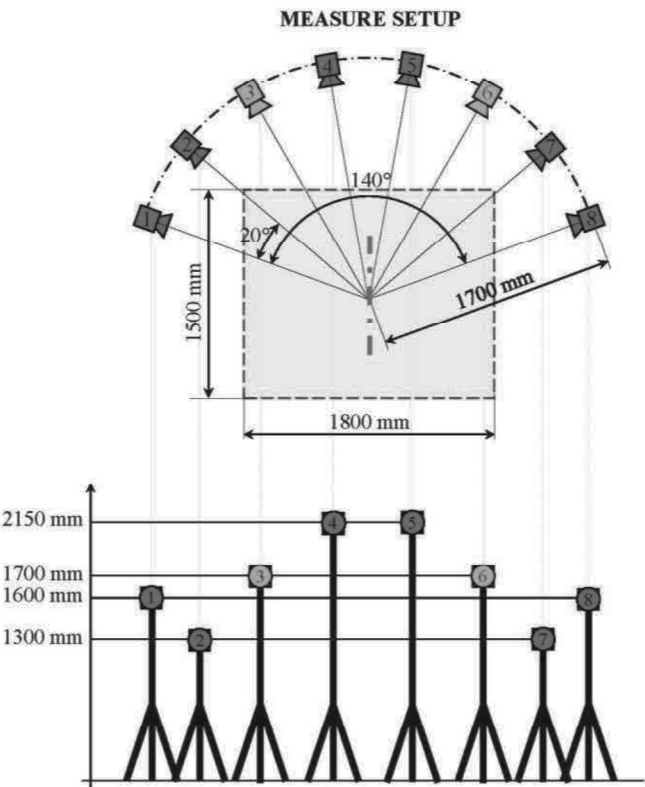
Figure 1: Schematic representation of the measure (top and frontal views, a) and gait (top view, b) setups. Bonita and Vero cameras are represented in blue and green, respectively. The grey rectangle represents the planar projection of the CV. The CV height is 1500 mm for both setups, with centre 840 mm and 750 mm above the ground for the measure and the gait setup, respectively. The blue dashed line represents the location and orientation of the pendulum rotation axis during the dynamic tests.

Figure 2: The tracking object with its principal dimensions, mounted on the rotor for an un-occluded (a) and occluded (b) dynamic test. Inter-marker distance between marker M1 and marker M2 was measured via laser scanner. The arc in (b) shows the trajectory of M2: with respect to a camera placed in front of the pendulum, red denote total occlusion and blue no occlusion, while the angular values denote transition between the two states and thus partial occlusion. Different cameras see the pendulum from different point of view, experiencing total, partial and no-occlusion at different angles.

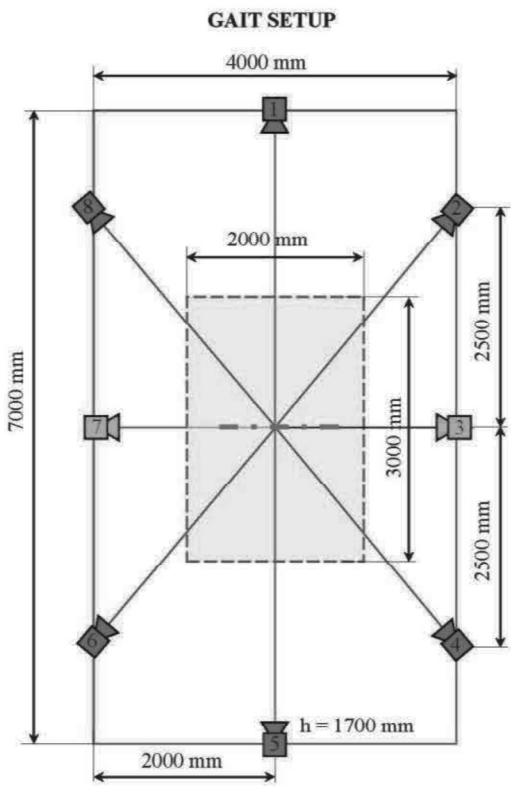
Figure 3: Variation of IMD error versus the pendulum rotation angle, 0° being the resting position, for the two setups. In all figures, all five trials are plotted together. In (a) and (b), the IMD error of occluded (red) and un-occluded (blue) motions are compared. In (c) and (d), the effects of a Butterworth with 4.5 Hz cut-off frequencies (orange) is compared with the unfiltered occluded motion (red). Similarly, in (e) and (f) the effects of a Butterworth filter with 15 Hz cut-off frequencies (purple) is compared with the unfiltered occluded motion (red).

Figure 4: Variation of IMD versus the pendulum rotation angle, 0° being the resting position, for a single pendulum oscillation, in case of total marker occlusions only (blue) or in case of combined total and partial marker occlusions (red) considering all cameras.

1 **FIGURE 1 (double column)**
2



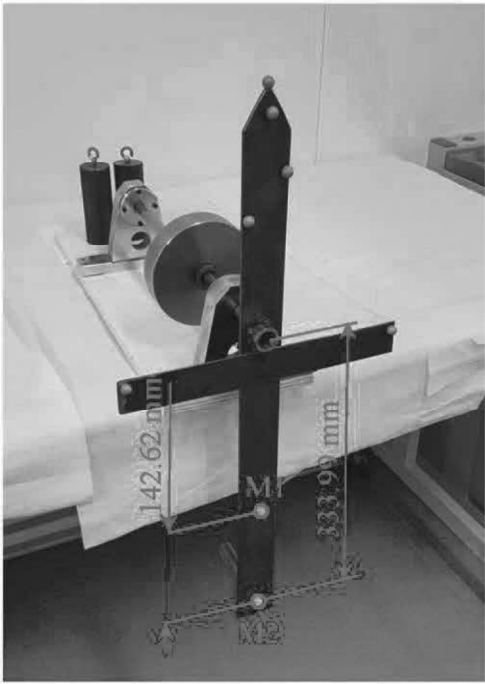
(a)



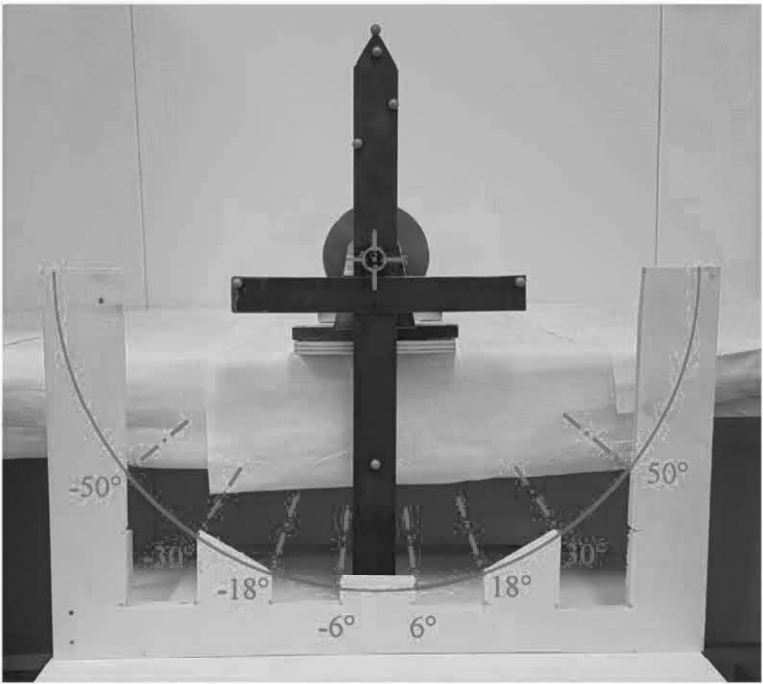
(b)

1 **FIGURE 2 (double column)**

2



(a)



(b)

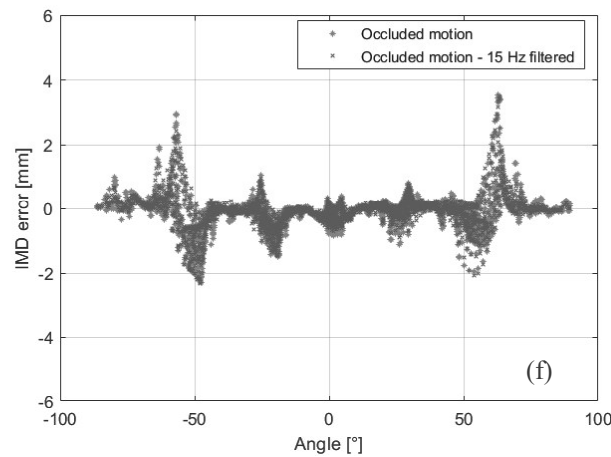
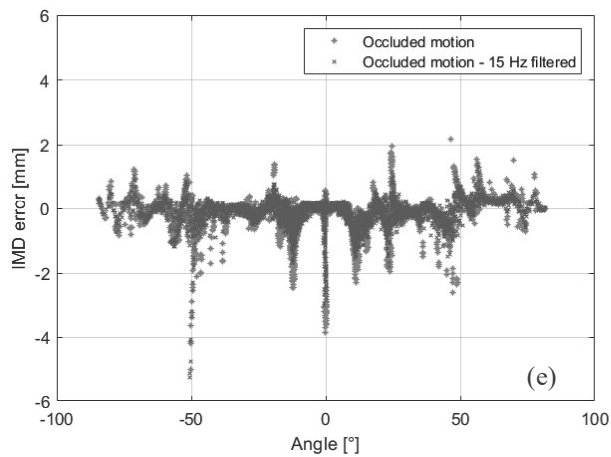
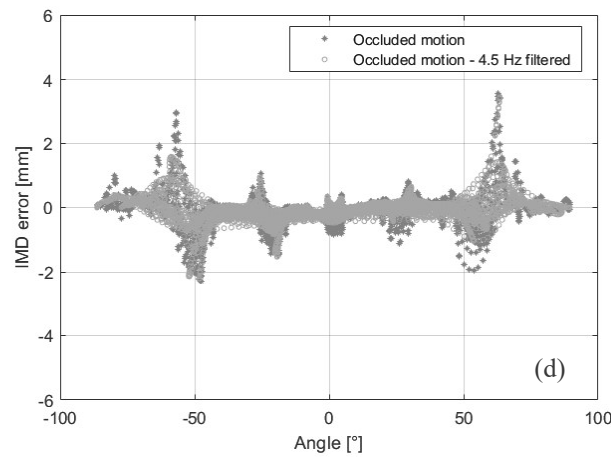
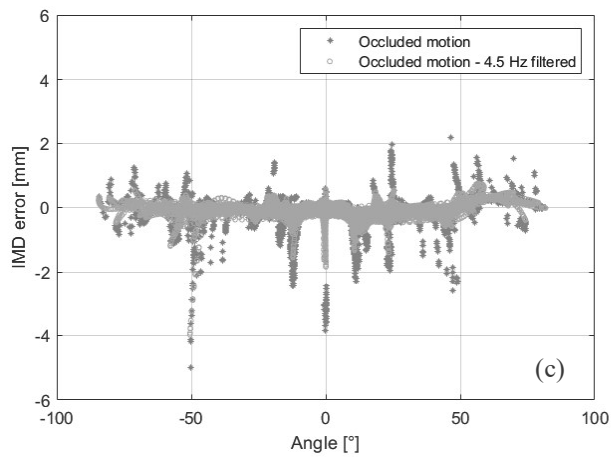
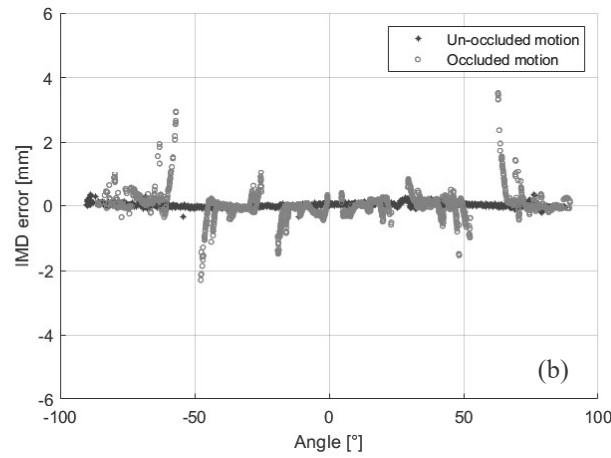
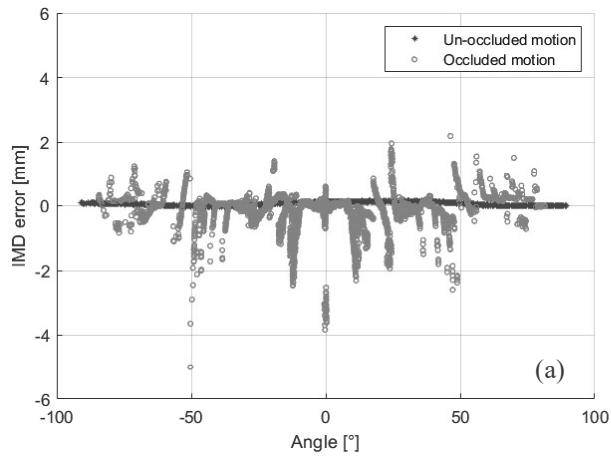
3

4

1 **FIGURE 3 (double column)**

2 **MEASURE SETUP**

GAIT SETUP



3

4

5

6

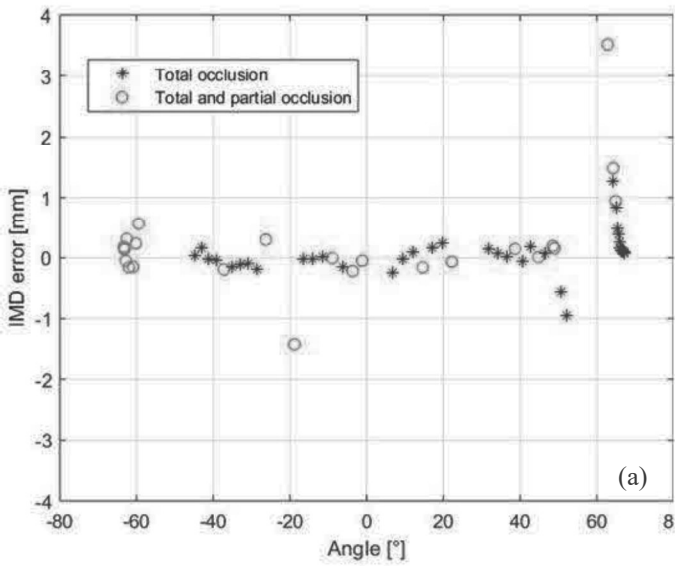
7

8

9

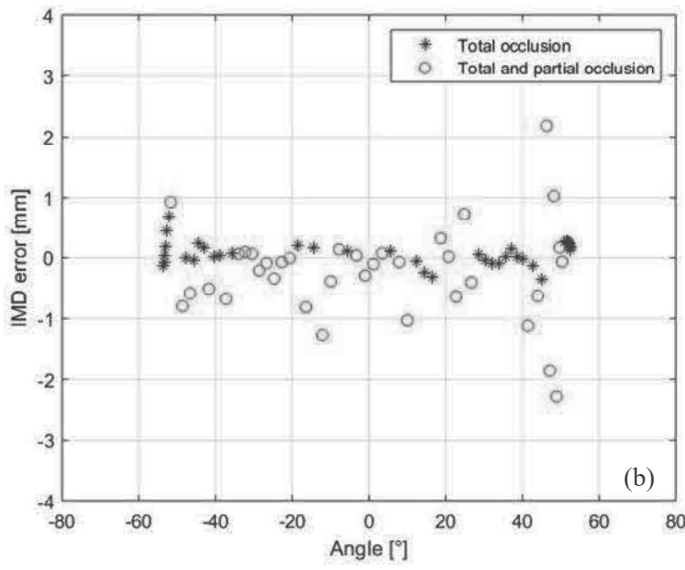
1 **FIGURE 4**

2 **MEASURE SETUP**



3

GAIT SETUP



1 Table 1: Performances of different OSSs in terms of accuracy and maximum error as reported in the literature.

Paper	OSS	Measure adopted	Accuracy definition	Accuracy value	Maximum error definition	Maximum error value
Ehara et al., 1997	Vicon 140, 4 cameras	Known distance	Mean absolute error	1.60±1.82 mm	Maximum distance variation	10.87 mm
	Vicon 370, 6 cameras			0.94±0.39 mm		12.94 mm
	Ariel APAS, 2 cameras			11.61±5.36 mm		37.54 mm
	Dynas 30/h, 2 cameras			18.42± 0.24 mm		78.68 mm
	ELITE PLUS, 4 cameras			0.53± 0.31 mm		2.15 mm
	Expert Vision, 4 cameras			1.14± 0.53 mm		12.22 mm
	PEAK5, 2 cameras			3.85± 2.04 mm		18.49 mm
	PRIMAS, 2 cameras			1.79± 0.14 mm		10.23 mm
	Quick MAG, 2 cameras			2.25± 0.52 mm		14.58 mm
	Video Locus Color, 2 cameras			7.63± 2.81 mm		41.81 mm
	Video Locus Reflective, 2 cameras			7.73± 1.45 mm		35.42 mm
Richards, 1999	VIcon 370	Known distance	Root mean squared error	0.62 mm	Max absolute error with no more than 3 cameras	5.57 mm
	Ariel APAS			4.27 mm		4.94 mm
	Chamwood CODA			4.87 mm		9.26 mm
	BTS Elite Plus			1.73 mm		16.13 mm
	Motion Analysis HiRes			0.59 mm		5.99 mm
	Qualisys ProReflex			0.80 mm		12.76 mm
	Peak Perform. Motus			0.91 mm		5.82 mm
Miller et al., 2002	Motion Analysis, six cameras	Known displacement	Mean absolute error	0.05 mm	--	--
Liu et al., 2007	Qualisys ProReflex-MCU120, two camers	Known displacement	--	--	Maximum error	± 4.25 µm
Windolf et al., 2008	Vicon-460, 4 cameras	Known displacement	Root mean squared error	63±5µm	Maximum grid-point error	416±129µm

Kuxhauset al., 2009	Vicon M-612 ViconPeak, 6 cameras, Vicon Workstation v4.5	Known displacement	Mean absolute error	0.05±0.005 mm.	Maximum absolute error	3.7 mm
Yang et al., 2012	Vicon MX,F40 cameras, 5 cameras, Nexus 1.6.1	Known displacement	Mean absolute error	<2 µm	Mean absolute error	<7 µm
Diaz Novo et al., 2014	Vicon MCam-60, 8 cameras, Vicon-Workstation V4.6	Known distance	--	--	Maximum mean error	< 5mm
	Vicon T160, 12 cameras, Vicon Nexus 1.7					< 5mm
	Canon Zr300, 3 cameras, Hu-m-an V5					<20 mm
Eichelberger et al., 2016	Vicon Bonita, 6 or 8 or 10 cameras, Vicon Nexus 1.8.5	Known distance	Mean error best case	0.08±0.05 mm	Mean error worst case	2.30± 0.001 mm
Morozov et al., 2016	Vicon T160	Absolute position	Mean absolute error	1.67 mm	Maximum mean absolute error	2.82 mm
Aurand et al., 2017	OptiTrack Prime 41, 42 cameras, OptiTrack Motive 1.10.1 Final software	Known displacement	Root mean squared error	<200 µm on 97% of the volume	Root mean squared error, worst case	<1mm
Di Marco et al., 2017	Vicon system MX-series, 8 cameras, Vicon Nexus 1.8.5	Known distance	3*STD of mean absolute error	0.1 mm	Maximum root mean squared error in dynamics	0.4 mm
	Vicon system T-series, 10 cameras, Vicon Nexus 1.8.5			0.3 mm		1.7 mm
Merriault et al., 2017	Vicon T40S, 8 cameras	Static- Known displacement Dynamics- Known distance	Static-mean absolute positioning error	0.15±0.015 mm.	Dynamics- Maximum error	< 2mm

1

2

Table 2: Accuracy of the two setups [mm] (mean values \pm standard deviation, computed over the averages) in case of: un-occluded cameras (first row); occluded cameras (aggregated data, second row); un-occluded cameras after occlusion tests (third row). Statistical analysis is reported in supplementary material.

	MEASURE SETUP	GAIT SETUP
All Cameras	0.05 ± 0.02	0.08 ± 0.01
Occluded Cameras	0.05 ± 0.04	0.11 ± 0.07
Post – All Cameras	0.05 ± 0.02	0.07 ± 0.01

Table 3: Mean values \pm standard deviation (computed over the averages) and maximum absolute marker displacement [mm] obtained during static tests for the two setups, in case of: repeated measure with un-occluded marker (first row); total marker occlusion to some cameras (second row); partial marker occlusion to some cameras (third row). Statistical analysis is reported in supplementary material.

	MEASURE SETUP		GAIT SETUP	
	Mean marker displacement	Maximum marker displacement	Mean marker displacement	Maximum marker displacement
System repeatability	0.12 ± 0.07	0.24	0.07 ± 0.04	0.13
Total marker occlusion	0.16 ± 0.09	0.44	0.18 ± 0.10	0.47
Partial marker occlusion	0.78 ± 0.43	1.73	1.21 ± 0.25	1.86

Table 4: Mean IMD absolute error (MIMDAE; mean value \pm standard deviation, computed over the averages) and maximum IMD variation [mm] in dynamic tests for the two setups, in case of: un-occluded tests (first row); occluded tests (second row); occluded tests with subsequent application of a Butterworth filter with two different cut-off frequencies (third and fourth row). Statistical analysis is reported in supplementary material.

	MEASURE SETUP		GAIT SETUP	
	MIMDAE	Maximum IMD variation	MIMDAE	Maximum IMD variation
Un-occluded motion	0.09 ± 0.00	0.20	0.05 ± 0.00	0.83
Occluded motion	0.26 ± 0.01	7.20	0.18 ± 0.00	5.82
Filtered occluded motion (4.5 Hz)	0.17 ± 0.01	4.73	0.22 ± 0.01	5.65
Filtered occluded motion (15 Hz)	0.22 ± 0.01	6.65	0.25 ± 0.01	6.21

1 **Table 5: IMD absolute error (mean value \pm standard deviation) and maximum IMD variation [mm] in the**
 2 **considered single pendulum oscillation during the dynamic tests for the two setups, computed over all**
 3 **measurements associated to: total marker occlusions only (first row); combination of total and partial marker**
 4 **occlusions (second row). Statistical analysis is reported in the supplementary material.**

	MEASURE SETUP		GAIT SETUP	
	IMD absolute error	Maximum IMD variation	IMD absolute error	Maximum IMD variation
Only total marker occlusion	0.16 \pm 0.13	1.05	0.18 \pm 0.24	1.52
Total and partial marker occlusion	0.56 \pm 0.60	4.47	0.46 \pm 0.78	4.94